Ocean and Sea Ice SAF

Scientific Report

SAF/OSI/CDOP3/KNMI/SCI/RP/313

Preliminary validation of the NSCAT-5 Geophysical model function

Wenming Lin

Marcos Portabella

Ad Stoffelen

Anton Verhoef

Zhixiong Wang

Version 1.3

1 November 2017

DOCUMENTATION CHANGE RECORD

Reference: **OSI_AVS_17_01**

Issue / Revision :	Date :	Change :	Description :
Version 1.0	2017-09-27	Wemming Lin	Draft version
Version 1.1	2017-10-08	Marcos Portabella	Revision
Version 1.2	2017-10-10	Anton Verhoef	Revision
Version 1.3	2017-11-01	Ad Stoffelen	Revision

Summary

Recent developments on the wind geophysical model function (GMF) of Ku-band scatterometers include a sea surface temperature (SST) dependent term. It has been found that the SST effects on the radar backscatter are wind speed dependent and more pronounced in vertical polarization (VV) than in horizontal polarisation (HH) at higher incidence angles, and are mainly relevant at radar wavelengths smaller than C-band. The new Ku-band GMF, NSCAT-5, is based on a physical model and RapidScat radar backscatter measurements, which are only available at two incidence angles, i.e., 48.8^0 and 55.2^0, for HH and VV beams, respectively. The aim of this study is to perform a preliminary verification of the NSCAT-5 GMF at similar incidence angles, using data from the recently-launched Indian SCATSat-1, which operates at 49.1^0 (HH) and 57.9^0 (VV) incidence angle. A more comprehensive validation will be carried out later in 2017, as part of a follow-on CDOP-3 VSA activity, including a more recent calibration version (1.2.3) and so-called stress-equivalent winds.

Contents

1 Introduction

The ocean normalized radar cross section (NRCS, σ^0) or backscatter measured by satellite scatterometer systems is representative of the sea surface roughness at the scale of gravity-capillary waves, which are dominated by mean sea-surface winds, but also modulated by some secondary geophysical effects, such as sea surface temperature (SST), increased wind variability [1] or (mainly for Ku-band systems) the presence of rain [2]. The radar backscatter is also a function of atmospheric and ocean mass density [3], the viewing geometry (incidence and azimuth angles), radar properties (polarization and frequency), and e.m. sea water properties, which are assumed constant here (no dependency on sea surface salinity, SSS).

Since the fundamental understanding of physical processes of the ocean surface backscatter is insufficient at the moment, empirical approaches are used to derive GMFs in practice. These GMFs give the radar backscatter as a function of several physical parameters, fitted to a large number of observations. Improving GMFs is a continuous effort and new versions are being developed over time, e.g., CMOD5 [4], C-2015 [5], and CMOD7 [6] for C-band, and for Ku-band SASS GMF [7], NSCAT-1 [8], NSCAT-4 [9], OSCAT GMF [10] and Ku-2011 [11]. GMF improvement is generally based on the analysis of wind and inversion residuals as a function of the GMF parameters, where the residuals may be obtained from the wind retrieval process or from comparison to reference wind data sets. However, wind and inversion residuals may also depend on parameters that are not yet part of the GMF, such as for example wind variability, waves, rain, or SST.

In [12] and [13], the variations of backscatter due to SST changes, depending on scatterometer radar frequency, polarization, and incidence angle, are investigated on the basis of a physics-based radar backscatter model and a dataset of collocated C-band (Advanced scatterometer or ASCAT) and Ku-band (RapidScat) scatterometer measurements. The study shows that the SST effects are substantial at Ku-band, but rather negligible for C-band backscatter measurements. Moreover, the SST effects are wind speed dependent and more pronounced in VV polarization and at higher incidence angles, the latter according to the physics-based backscatter model. While, the SSS effects (mainly corresponding to ocean mass density variations) on scatterometer winds are limited (within 1%). As a result, a new Ku-band GMF, NSCAT-5, which includes a SST-dependent term, has been developed.

Although it has only been verified for one incidence angle per polarization (48.8° for HH and 55.2° for VV) for RapidScat, NSCAT-5 actually models the sensitivity of the Ku-band radar backscatter to sea surface wind for a wide range of incidence angles from 22° to 59°. Therefore, the question remains as to what is the accuracy of the new GMF for other instruments at other incidence angles?

The ISRO SCATSat-1 satellite was launched in September 2016, carrying onboard a pencil-beam rotating scatterometer, similar to its predecessors SeaWinds on QuikSCAT and ADEOS-2, Oceansat-2, HY-2A, and RapidSCAT. The SCATSat-1 viewing geometry is slightly different from that of RapidScat. For instance, the incidence angles for the HH and VV beams are 49.1° ±0.4° and 57.9° ±0.4°, respectively. As such, SCATSat-1 radar backscatter data can be used to verify the NSCAT-5 GMF at two incidence angles used to fit the SST-dependence term, i.e., 48.8° (for

HH) and 55.2° (for VV). Moreover, SCATSat-1 follows a sun-synchronous polar orbit, thus also dwelling over cold polar waters.

In this study, a similar approach to [13] is carried out to analyse the sensitivity of SCATSat-1 radar backscatter to SST under different wind conditions. Section 2 describes the used data sets. Section 3 presents the binning procedure and the potential biases between different wind sources. In Section 4, the SST dependency in SCATScat backscatter measurements is addressed. Finally, the conclusions and the outlook are presented in section 5.

2 Data

Two months (February - March 2017) of collocated ASCAT-A (onboard Metop-A satellite) 25-km Level 2 (L2) winds and SCATSat-1 scatterometer winds are analyzed. Both data sets are in Binary Universal Format Representation (BUFR), and are provided by the European Organisation for the Exploitation of Meteorological Satellites (EUMETSAT) Ocean and Sea Ice (OSI) Satellite Application Facility (SAF). The scatterometer data sets already include collocated European Centre for Medium-range Weather Forecasts (ECMWF) model wind output, which are estimated by interpolating three ECMWF 3-hourly forecast winds on a 62.5-km grid both spatially and temporally to the scatterometer data acquisition location and time, respectively. The SCATSat-1 winds are processed with the Level 2A (L2A) version 1.1.2 (v1.1.2) backscatter (σ^0) "egg" data, using the NWP SAF Pencil-beam scatterometer Wind Processor (PenWP) with the NSCAT-4 GMF [14]. A σ^0-dependent correction for σ^0 values above -19 dB is used to correct for increasing wind speed biases above ~15 m/s due to the non-linearity in the backscatter values. Then a constant correction of 0.61 dB / -0.03 dB for the HH/VV beams is applied to bring the average signal levels to the model values (using ECMWF winds as input) and to minimise wind speed biases. The ASCAT winds are reprocessed using the ASCAT Wind Data Processor (AWDP) with the CMOD7 GMF [6], which is based on a combination of CMOD5.N and C2013 (particularly for low winds) [15][16][17], and has been constrained to provide a uniform wind speed probability density function (PDF) over the entire swaths of ASCAT and ERS. Air mass density variations are ignored in this preliminary study, but since these are latitude dependent too, just like SST, the next version SCATSat-1 winds (v1.1.3) collocated with ASCAT, will be supplemented by ECMWF stress-equivalent 10-meter winds [3].

The collocation criteria are less than 30 minutes distance in time and 25 km distance in space between SCATSat-1 and ASCAT measurements. Note that all SCATSat-1 winds across the swath are used in analysis. The total amount of collocations is about 8.4 million, with 7.9 million quality-control (QC) accepted data. Figure 1(a) illustrates the geographical distribution of the collocated ASCAT-SCATSat data, while Figure 1(b) shows the two-dimensional histogram of the collocations as a function of temporal (*y*-axis) and spatial (*x*-axis) distances.

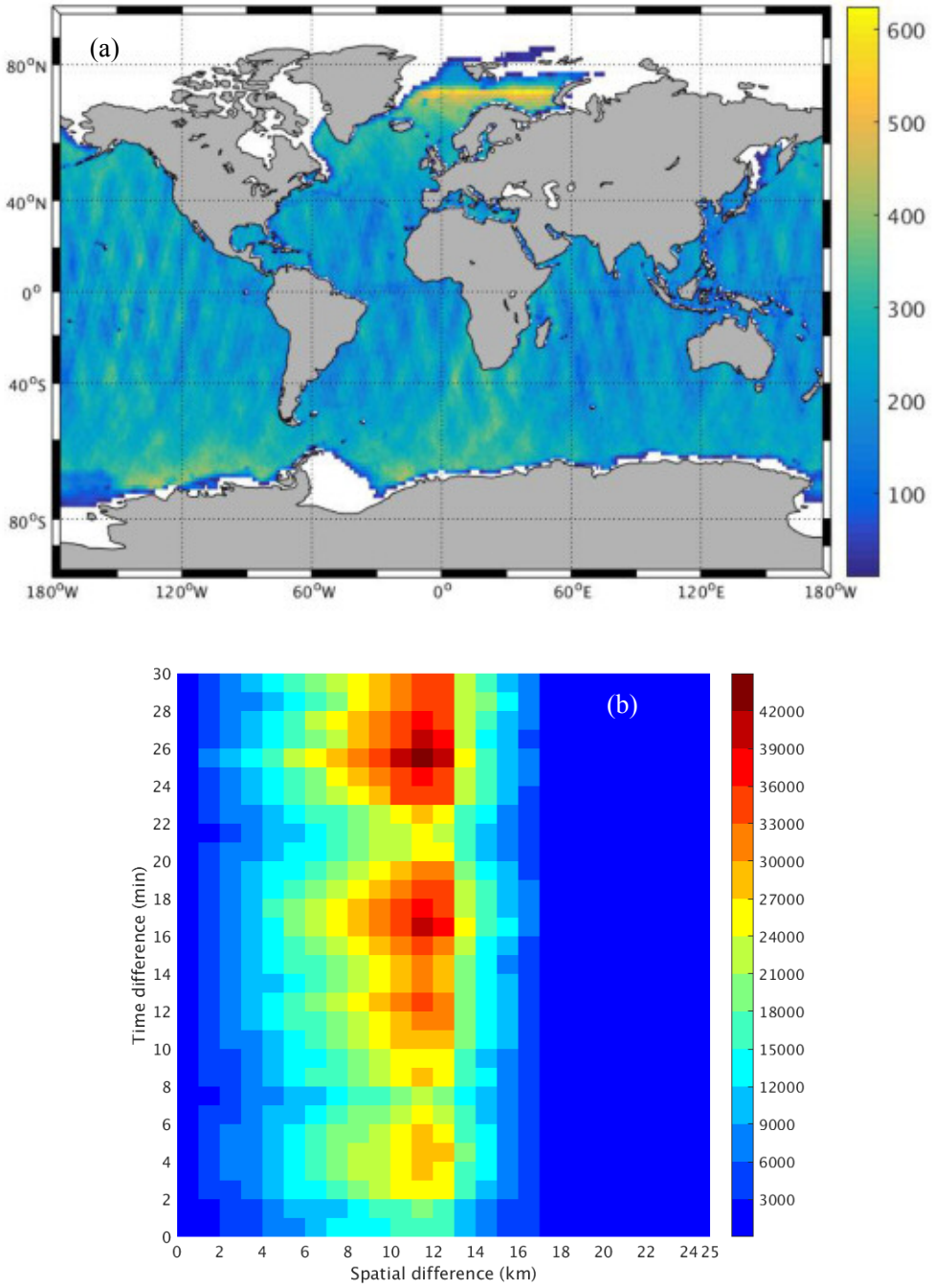

Fig. 1 (a) The geographical distribution of the collocated ASCAT-SCATSat data, latitude and longitude bins of 1°; (b) Two-dimensional histogram of the collocations as a function of temporal and spatial distances, bins of 1 minute and 1 km respectively.

3 Analysis of wind speed differences

In practice, the SST dependency of the Ku-band backscatter is derived from the analysis of binned observations and simulations. Following [13], ASCAT winds are considered to be independent of SST, and are therefore used as reference.

Figure 2 shows the mean wind speed differences between the three data sources (i.e., ASCAT, SCATSat, and ECMWF) as a function of the averaged wind speed. Note that all combinations show systematic differences as a function of wind speed. In particular, these are smaller for the ASCAT/ECMWF pair (notably at medium and high winds).

An extension of the wind speed differences to the SST dependency is shown Fig. 3. In particular, panels (a) and (b) show the mean wind speed differences between ASCAT and ECMWF and between SCATSat and ECMWF, respectively, as a function of averaged wind speed and SST. The black curve depicts the mean SST value at each averaged speed bin. Panels (c) and (d) show the same as (a) and (b), respectively, but for the standard deviation of the wind speed differences.

Note that these wind speed differences may be caused by both scatterometer and ECMWF wind errors. For example, the differences at high SST values are associated with the Intertropical Convergence Zone (ITCZ) and moist convection, in which case the Ku-band scatterometer is more likely to be affected by water vapour or rain than the C-band scatterometer. On the other hand, deep moist convection in the Tropics increases the surface wind variability. This phenomenon is not well resolved by the ECMWF model, leading to large background wind errors. As such, other geophysical conditions could be inadvertently associated with SST, and in turn, generate apparent SST-dependent bias. Consequently, a speed-dependent bias correction is applied to ASCAT winds in order to match the C- and Ku-band speed distributions. The correction factor is formulated as

$$\Delta V_{SA} = \overline{V_S - V_A}(v) \tag{1}$$

where ΔV_{SA} is the mean speed difference between SCATSat (V_S) and ASCAT (V_A) winds as a function of the averaged speed v. The corrected ASCAT wind speed is then

$$V_A' = V_A + \Delta V_{SA}(V_A) \tag{2}$$

with the remaining speed difference defined as

$$\Delta V_{SA}' = V_S - V_A' \tag{3}$$

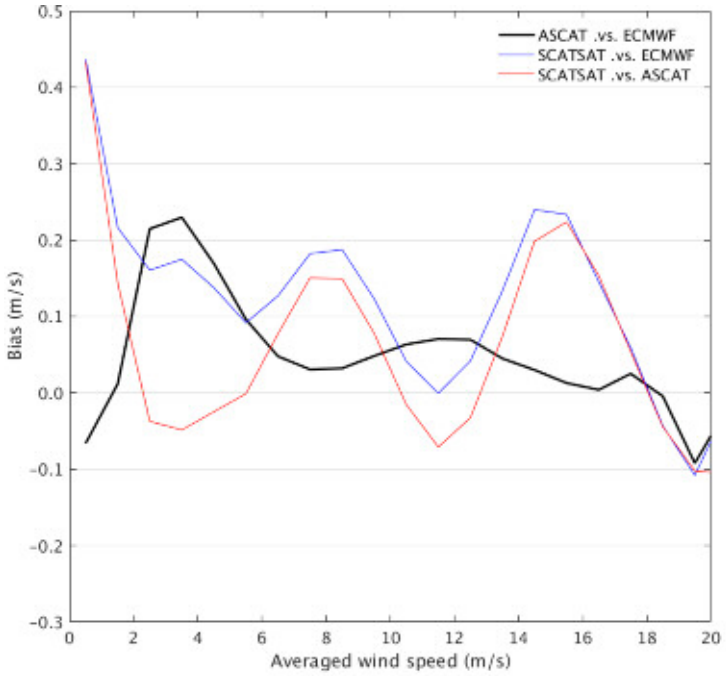

Fig. 2 Mean wind speed difference between ASCAT and ECMWF (black curve), SCATSat and ECMWF (blue curve), and SCATSat and ASCAT (red curve), as a function of the averaged wind speed of each pair of wind sources, with a binning of 1 m/s.

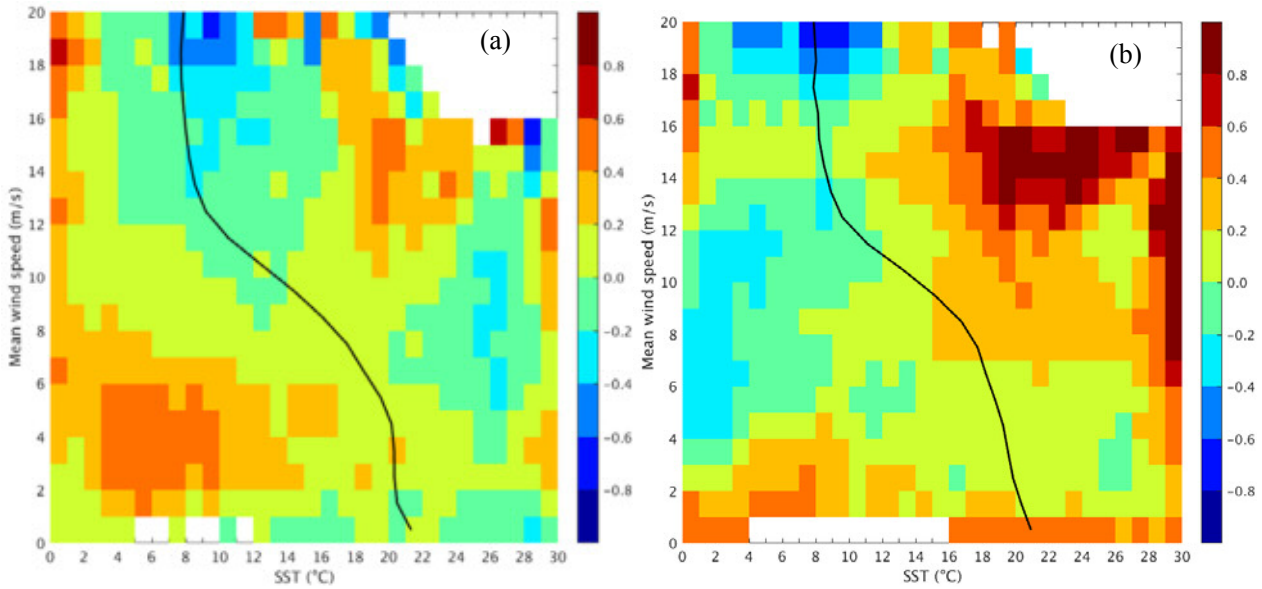

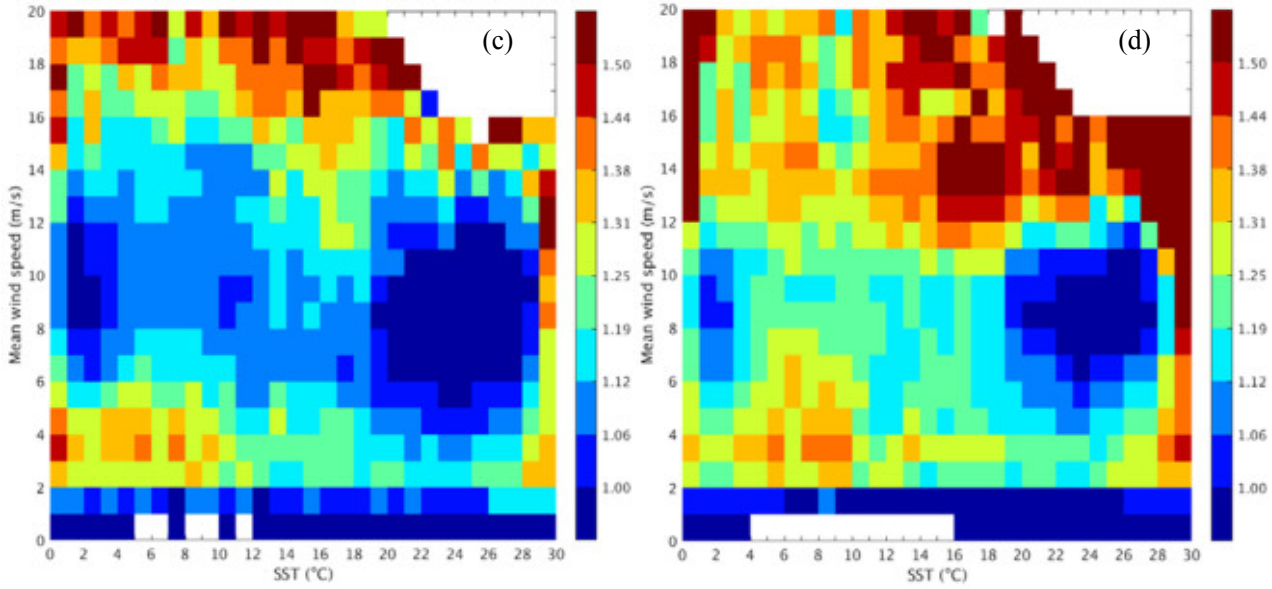

Fig. 3 Mean wind speed difference (m/s) between ASCAT and ECMWF (a) and between SCATSat and ECMWF (b) as a function of averaged wind speed and SST. The black curves depict the mean SST at each wind speed bin. Panels (c) and (d) present the standard deviation of the differences between ASCAT and ECMWF winds, and between SCATSat and ECMWF winds, respectively.

Figure 4 shows $\Delta V'_{SA}$ as a function of average wind speed. In contrast with ΔV_{SA} (see red curve in Fig. 2), $\Delta V'_{SA}$ is (by construction) only marginally dependent on wind speed.

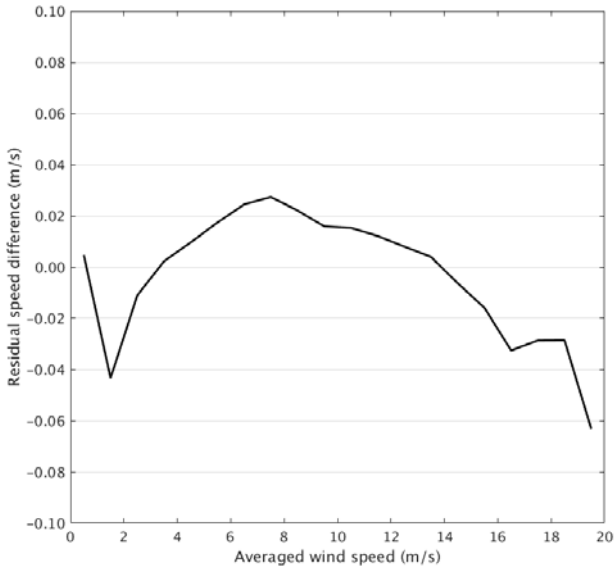

Fig. 4 Mean wind speed difference between SCATSat-1 and the corrected ASCAT winds

Figure 5 shows $\Delta V'_{SA}$ as a function of (a) average wind speed (i.e., the average of V'_A and V_S) and relative wind direction (i.e., the ASCAT wind direction w.r.t. the SCATSat first beam pointing), (b) SST and relative wind direction, and (c) SST and wind speed. Since $\Delta V'_{SA}$ is rather independent on wind speed (see Fig. 4), it is clear from Fig. 5 that the SST impact on the wind speed difference is the largest, followed by the wind direction. SST induces different errors on the VV and HH GMFs

[12], which are then compromised somehow in the nonlinear wind retrieval. Once the SST dependence is incorporated in the GMF, one may expect that the $\Delta V'_{SA}$ dependency on wind direction is also removed. Although the overall $\Delta V'_{SA}$ dependency on wind speed is small (see Fig. 4), it clearly shows up for different SST bins (Fig. 5(c)). Consequently, the wind speed is taken into account when modelling the improved GMF NSCAT-5 [13].

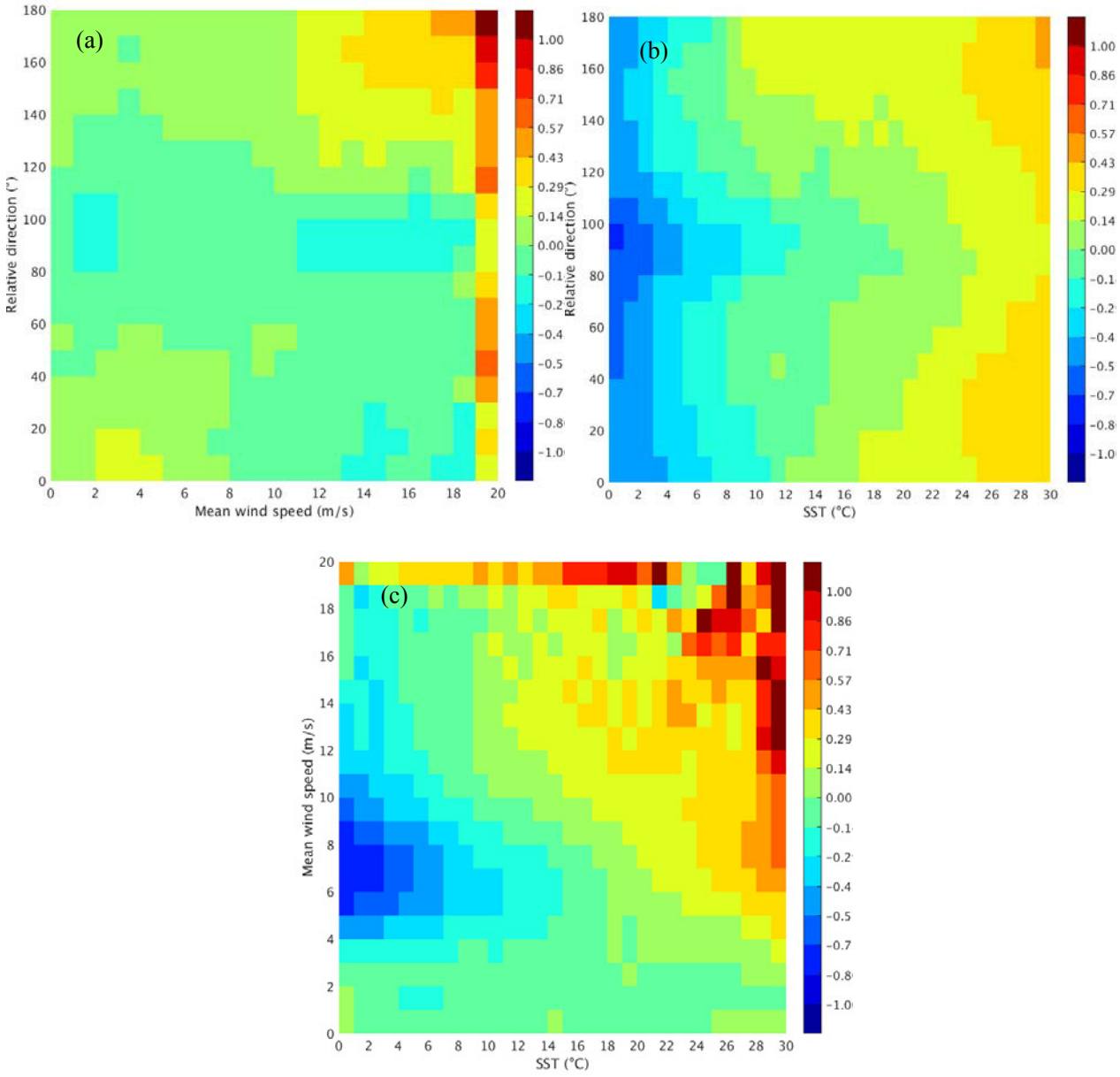

Fig. 5 $\Delta V'_{SA}$ as a function of (a) average wind speed and relative wind direction (i.e., the ASCAT wind direction w.r.t. the first beam of SCATSat); (b) SST and relative wind direction; (c) SST and wind speed. The wind speed, wind direction, and SST are binned every 1 m/s, 10°, and 1°C respectively.

4 SST dependence analysis

The observed SCATSat backscatter values at wind speed $V = \frac{1}{2}(V_A' + V_S)$ and SST T are denoted as $\sigma^0_{p,obs}(V,T)$. The simulated backscatters using NSCAT-4 and SCATScat observation geometry are denoted as $\sigma^0_{p,sim}(V,T) = \sigma^0_{p,sim}(V_A', T_{GMF})$. T_{GMF} is determined by the mean SST of the sea surface measurements which were used to derive NSCAT-4 [8]. As shown in Fig. 3 (solid curve), T_{GMF} is actually a function of wind speed. Figure 6 shows the mean observed and simulated backscatter values as a function of SST for the wind speed range 5.5 m/s<V<6 m/s. As expected, the simulated backscatter values show no significant dependence on SST, indicating that the SCATScat sampling is similar to that of the NASA Scatterometer (NSCAT), which was used to derive the NSCAT-4 GMF. However, the real backscatter measurements (solid lines) show a clear SST dependence, more pronounced in VV (red) than in HH (black).

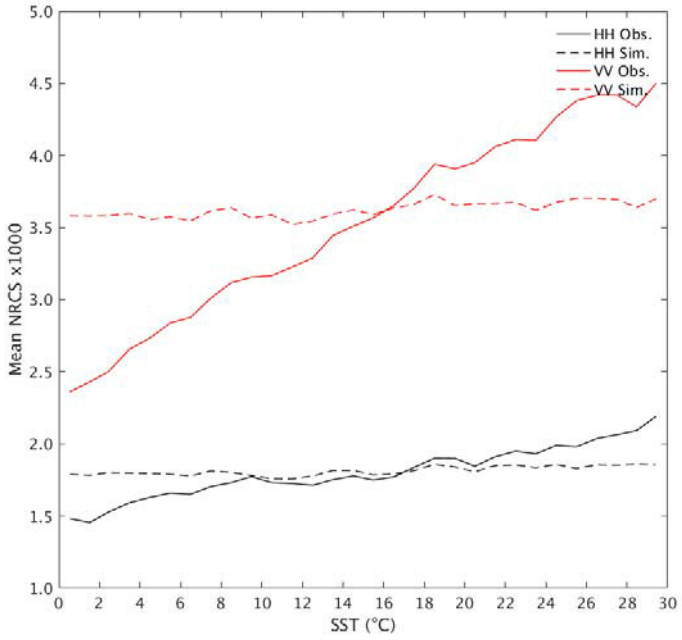

Fig. 6 The mean observed and simulated NRCS (value times 1000) as a function of SST for wind speed of 5.5 m/s<V<6 m/s. The black curves are for HH polarisation and the red curves for VV polarisation.

Consequently, one may expect that the improved NSCAT-5 model (*abbr.* N_5) that includes SST dependency can be easily derived from NSCAT-4 (*abbr.* N_4) by applying the following correction:

$$GMF_{N5} = f_p(V,T) \times GMF_{N4} \tag{4}$$

where

$$f_p(V,T) = \frac{\sigma^0_{p,obs}(V,T)}{\sigma^0_{p,sim}(V,T)} \tag{5}$$

Figure 7 shows f_{VV} and f_{HH} as a function of SST, for several wind speed bins. The absolute variations of σ^0 as given by $f_p(V,T)$ may be shifted due to statistical wind speed biases and may have different scaling at various wind speeds, because T_{GMF} varies with V for NSCAT-4. In consequence, $f_p(V,T)$ is further normalized by its value at certain reference SST T_0, e.g., T_0=12.5°C, such that,

$$g_p(V,T) = \frac{f_p(V,T)}{f_p(V,T_0)} \tag{6}$$

Fig. 8 illustrates the same curves as Fig. 7 but for g_p. It is clear that the SST dependency in both VV and HH polarisations is more pronounced at low and medium wind speeds (V < 10 m/s) than at high wind speeds (V > 10 m/s). For SST above 25 °C and high wind speeds (V > 10 m/s), the correction factor slightly decreases for VV polarisation, while it sharply increases for HH polarisation. This is connected to quality control (QC) issues, e.g., the moist convection over Tropics, which are further looked into. Since Ku-band scatterometers are very sensitive to rain, it is not easy to decouple rain from high wind speeds based on the current wind quality control (QC). In other words, it is also difficult to decouple SST effects from other geophysical conditions. A more rigorous QC could be used to remove as much rain-contaminated data as possible, such that a more confident derivation of NSCAT-5 at high wind speeds can be achieved. However, due to the current lack of data, it is not straightforward to fit the curves in Fig. 7 or Fig. 8 in order to derive the coefficients of the Taylor expansion of $f_p(V,T)$.

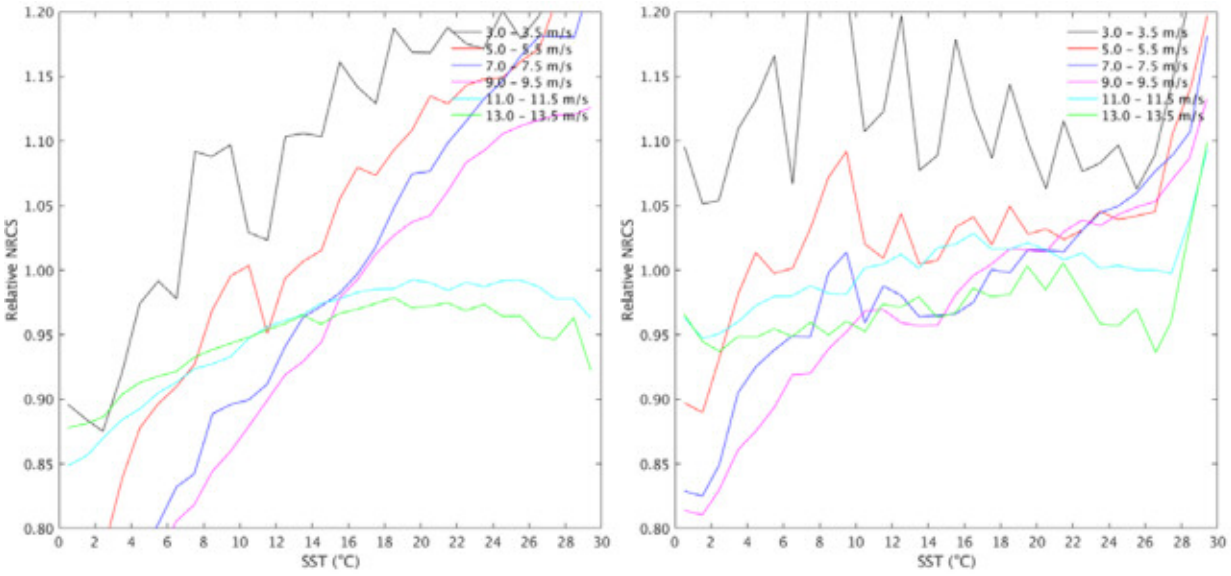

Fig. 7 f_{VV} (a) and f_{HH} (b) as a function of SST, and for certain wind speed bins (see the legends).

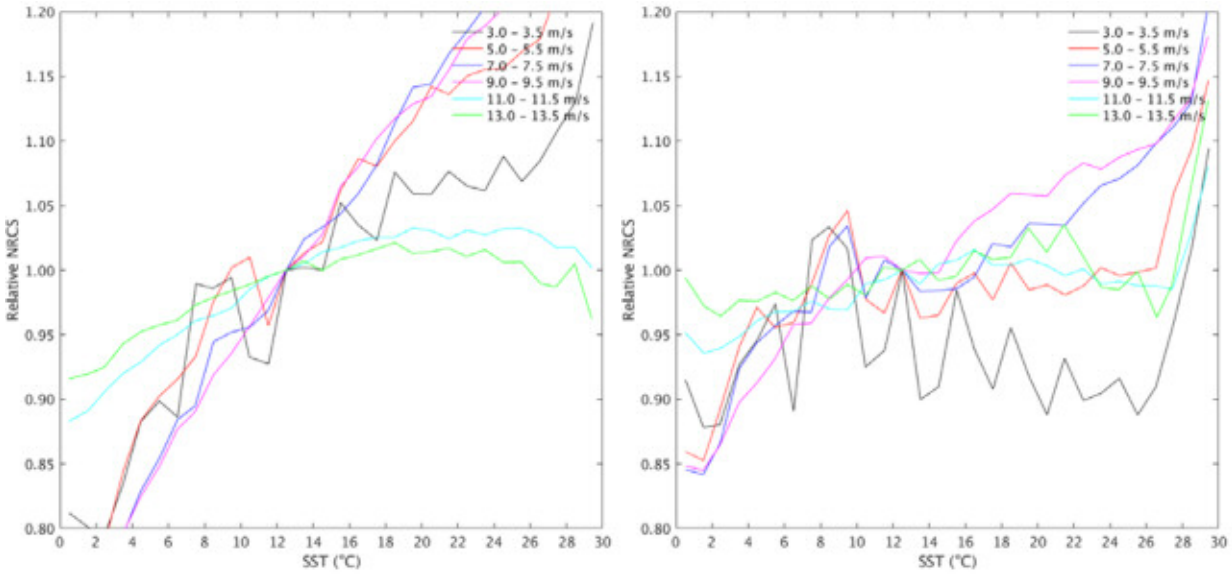

Fig. 8 Same as Fig. 6 but for g_{VV} (a) and g_{HH} (b).

5 Conclusions

In this study, the approach used to derive the NSCAT-5 GMF for RapidScat is adapted to assess SCATSat-1 backscatter sensitivity to sea surface wind and SST, both for HH and VV polarisations. The ASCAT winds are used as reference in the analysis. Most of the results are similar to those in [12], except that: 1) the wind speed difference dependency on relative wind direction is substantially lower in Figures 4(a) and (b) than those in [12]; 2) unlike [12], we do not find any SST dependency in the simulated backscatter values in Fig. 5. These may be attributed to the different sampling between RapidScat and SCATSat-1 scatterometer. Also, in Fig. 7(a), the decrease of $g_p(V,T)$ at high winds is not seen with RapidScat data. This may be due to remaining rain contaminated data in the QC-accepted SCATScat data. A more rigorous QC will be tested soon. Moreover, the effect of stress-equivalent winds will be assessed.

In the next phase of this study, more data will be used to derive the correction factor $g_p(V,T)$. In particular, the Scatsat-1 data will be reprocessed with PenWP and NSCAT-5 GMF (derived the [12]), then the MLEs from Scatsat-1 and RapidScat in the same latitudinal band (i.e., that of Rapidscat) and period of time (same month(s) even if for different years) will be compared. Finally, the SCATSat-1 QC will be tuned to match that of RapidScat, accounting for the above MLE analysis. Since, air mass density is latitude dependent, the next version SCATSat-1 winds (v1.1.3) collocated with ASCAT, will be supplemented by ECMWF stress-equivalent winds for comparison to NSCAT-5 [3].

Acknowledgments

The work has been funded under the EUMETSAT Ocean and Sea Ice (OSI) Satellite Application Facility (SAF) Associated Scientist project (reference OSI_AVS_17_01). We acknowledge ISRO for putting the SCATSat-1 data available. The ASCAT and SCATSat-1 scatterometer winds are

provided by EUMETSAT. The software used in this work has been developed through the EUMETSAT Numerical Weather Prediction SAF. The ECMWF data are retrieved from the ECMWF MARS archive.

Acronyms and abbreviations

Table 4 – List of acronyms and abbreviations

Name	Description
ASCAT	Advanced scatterometer
AWDP	ASCAT Wind Data Processor
BUFR	Binary Universal Form for Representation (of meteorological data)
CMOD	C-band geophysical model function used for ERS and ASCAT
CSIC	Consejo Superior de Investigaciones Científicas
ECMWF	European Centre for Medium-Range Weather Forecasts
ERS	European Remote sensing Satellite
ESA	European Space Agency
EUMETSAT	European Organization for the Exploitation of Meteorological Satellites
GMF	Geophysical Model Function
KNMI	Koninklijk Nederlands Meteorologisch Instituut (Royal Netherlands Meteorological Institute)
METOP	Meteorological Operational satellite
MLE	Maximum likelihood estimator
NWP	Numerical Weather Prediction
OSI	Ocean and Sea Ice
QC	Quality Control
RR	Rain rate
SA	Singularity Analysis
SAF	Satellite Application Facility
SD	Standard Deviation
SE	Singularity Exponent
WVC	Wind Vector Cell

References

[1] Lin, W., Portabella, M., Stoffelen, A., Verhoef, A., and Turiel, A., "ASCAT wind quality control near rain," *IEEE Trans. Geosci. Rem. Sens.*, 53 (8), pp. 4165-4177, 2015.

[2]Portabella, M., and Stoffelen, A., "Rain detection and quality control of SeaWinds," *J. Atm. and Ocean Techn.*, 18 (7), pp. 1171-1183, 2001.

[3] Kloe, Jos de, Ad Stoffelen, and Anton Verhoef, Improved Use of Scatterometer Measurements by Using Stress-Equivalent Reference Winds, *IEEE J. Sel. Top. Appl. Earth Obs. Remote Sens.,* 10, (5), 2017, DOI: 10.1109/JSTARS.2017.2685242.

[4] Hersbach, H., Stoffelen, A., and De Haan, S., "An improved C-band scatterometer ocean geophysical model function: CMOD5", *J. Geophys. Res. Oceans*, 112(C3), 2007.

[5] Ricciadulli, L., "ASCAT on MetOp-A data product update notes", *RSS Tech. Report 040416*, Remote Sensing System, 2016.

[6] Stoffelen, A., Verspeek, J., Vogelzang, J., and Verhoef, A., "The CMOD7 Geophysical Model Function for ASCAT and ERS Wind Retrievals," *IEEE J. Sel. Top. Appl. Earth Obs. Remote Sens.*, 10(5), 2123-2134, 2017.

[7] Wentz, F. J., Peteherych, S., and Thomas, L. A., "A model function for ocean radar cross sections at 14.6 GHz,", *J. Geophys. Res. Oceans*, 89(C3), 3689-3704, 1984.

[8] Wentz, F. J., and Smith, D. K., "A model function for the ocean-normalized radar cross section at 14 GHz derived from NSCAT observations," *J. Geophys. Res. Oceans*, 104, 11499-11514, 1999.

[9] OSI SAF, Algorithm Theoretical Basis Document for the OSI SAF wind products, SAF/OSI/CDOP2/KNMI/SCI/MA/197, and "NSCAT-4 Geophysical Model Function", 2014. Available at http://projects.knmi.nl/scatterometer/nscat_gmf/ .

[10] Gohil, B. S., Sikhakolli, R., and Gangwar, R. K., "Development of geophysical model functions for Oceansat-2 scatterometer," IEEE Geoscience and Remote Sensing Letters, 10(2), 377-380, 2014.

[11] Ricciardulli, L., and Wentz, F. J., "A scatterometer geophysical model function for climate quality winds: QuikSCAT Ku-2011," *Journal of Atmospheric and Oceanic Technology*, 32(10), 1829-1846, 2015.

[12] Wang, Z., Stoffelen, A., Fois, F., Verhoef, A., Zhao, C., Lin, M., and Chen, G., "SST dependence of Ku- and C-band backscatter measurements," *IEEE J. Sel. Top. Appl. Earth Obs. Remote Sens.*, Vol. 10, no.5, pp. xx1-12, 2017.

[13] Wang, Z., Stoffelen, A., Zhao, C., Vogelzang, J. Verhoef, A., Verspeek, J., Lin, M., and Chen, G., "A SST-dependent Ku-band geophysical model function for RapidScat," *J. Geophys. Res. Oceans,*122(4), 3461-3480, 2017.

[14] Verhoef, A., Vogelzang, J., Verspeek, J., and Stoffelen, A., "PenWP user manual and reference guide," NWPSAF-KN-UD-009, Version 2.1, KNMI, De Bilt, the Netherlands, Feb. 2017.

[15] Hersbach, H., "CMOD5.n: A C-band geophysical model function for equivalent neutral wind," ECMW F technical memorandum. [Online]. Available: http://www.ecmwf.int/sites/default/files/elibrary/2008/9873-cmod5n-c-band-geophysical-model-function-equivalent-neutral-wind.pdf.

[16] Verhoef, A., Portabella, M., and Stoffelen, A., "CMOD5.n – The CMOD5 GMF for neutral winds," SA F/OSI/CDOP/KNMI/TEC/TN/165. [online]. Available: http://projects.knmi/nl/publications/fulltexts/cmod5_neutral_winds_1.0.pdf

[17] Ricciardulli, L., and Wentz, F., "Towards a climate data record of ocean vector winds: The new RSS AS CAT," in Proc. Int. Ocean Vector Wind Sci. Team Meet., Knona, HI, USA, May 2013. [Online]. Available: http://coaps.fsu.edu/scatterometry/meeting/docs/2013/New_Products/Ricciardulli_ovwst_2013_ascat_winds_updated.pdf.